Simulation of Wiped Film Evaporator

Adil A. Al-Hemiri[*], Emad F. Mansour [**] and Jamal A.L. Al-Ani [**]

[*]*Chemical Engineering Department, College of Engineering, University of Baghdad.*
[**] *Chemistry and Petrochemical Industries Research Administration, Ministry of Science and Technology.*

Abstract

A mathematical model and associated computer program were developed to simulate the steady state operation of wiped film evaporators for the concentration of glycerol-water solution. In this model, various assumptions were made to facilitate the mathematical model of the wiped film evaporator. The fundamental phenomena described were: sensible heating of the solution and vaporization of water. Physical property data were coded into the computer program, which performs the calculations of this model. Randomly selected experiments were carried out in a small scale wiped film evaporator from ALVAL COMPANY, using different concentrations of the glycerol solution (10, 30 and 50 Wt. %) for different feed rates (30, 50, 80, 100 and 120 l/h) and two values of steam jacket pressure (2 and 4 atm) to compare between experimental and simulation results. The statistical analysis gave correlation coefficient of 0.9972, average absolute error of 2.2527 % and F-test of 0.9639 which showed the high accuracy of the simulation work.

Keywords: Wiped film evaporator, Evaporators, Simulation of film evaporators

Introduction

Evaporation is one of the main methods used in chemical industry for concentration of aqueous solutions that means the removal of water from solution by boiling the liquor in a suitable type of evaporator and withdrawing the vapor (Coulson & Richardson,1983). The objective of evaporation is to concentrate a solution consisting of non-volatile solute and a volatile solvent. In the overwhelming majority of evaporations the solvent is water. Normally, in evaporation the thick liquor is the valuable product and the vapor is condensed and discarded.

Agitated thin film evaporators, wiped film evaporators, are designed to spread a thin layer or film of liquid on one side of a metallic surface, with heat supplied to the other side. The unique feature of this equipment is not the thin film itself, falling and rising-film evaporators use thin liquid layers, but rather the mechanical agitator device for producing and agitating the film (APV, 2000).

Conventional heat transfer equipment may not be well suited for certain evaporation applications, particularly those involving heat sensitive products, viscous material or chemical constituents that exhibit fouling or foaming tendencies. For products like these, mechanically agitated thin-film evaporators are often selected over more conventional evaporators because of their batter process economics and performance (Mutzenburg, 1965).

For these applications, the heat transfer is not actually wiped or scraped but a highly agitated thin film is spread on to the metallic heat-transfer surface.

Agitation has the benefits in thin film equipment other than liquid turbulence. The blades assure even distribution of the liquid over the metal heat transfer surface; they eliminate any channeling of liquid as the liquid flows down the evaporator; the considerable shearing effect decreases the apparent viscosity of most liquids, thus improving internal heat and mass transfer (Parker, 1965). Also the heat transfer coefficient will be improved due to two reasons:

- Turbulence is included in the bulk of the fluid and near to the transfer surface reducing the effects of the resistance to heat transfer at the wall,

- Secondly where the surface is actually being scraped, the adhering film process liquid is constantly being

removed from the wall and distributed into the bulk of the liquid. At the same time fresh material is being presented to clean heat transfer surface.

The heat flux and the evaporation capacity are affected by changes both in temperature drop and in the overall heat transfer coefficient. The temperature drop is fixed by the properties of the steam and the boiling liquid and except for the effect of hydrostatic head is not a function of the evaporator construction. The overall heat transfer coefficient, on the other hand, is strongly influenced by the design and the method of operation of the evaporator. In most services, a well-designed and properly specified unit can achieve a heat flux of 31550-78875 W/m^2 when processing typical organic, and as high as 157750 W/m^2 in some aqueous applications (Abichandani et al , 1987).

The overall resistance to heat transfer between the steam and the boiling liquid is the sum of five individual resistances: the steam-film resistance; the two scale resistance, inside and outside the tubes; the tube wall resistance; and the resistance from the boiling liquid. The overall coefficient is represented by equation (1). In most evaporators the fouling factor of the condensing steam and the resistance of tube wall are very small, and they are usually neglected in evaporator calculation. In agitated-film evaporator the tube wall is fairly thick so that the resistance may be a significant part of the total ((Abichandani et al , 1987).

$$\frac{1}{U} = \frac{1}{h_o} + \frac{1}{h_i} + \frac{1}{\frac{K_w}{L_w}} + \frac{1}{\frac{K_o}{L_o}} + \frac{1}{\frac{K_i}{L_i}} \qquad (1)$$

Due to the difficulty of measuring the individual film coefficient in an evaporator, experimental results are usually expressed in terms of overall coefficients. These are based on the net temperature drop corrected for boiling-point elevation. The overall coefficient, of course, is influenced by the same factors influencing individual coefficients; but if one resistance (say, that of the liquid film) is controlling, large changes in the other resistance have almost no effect on the overall coefficient (Freese & Glover, 1979).

Freese & Glover, (1979), also, reviewed a number of wiped film evaporators pilot-plants test on typical solvent recovery application performed at atmospheric conditions with steam as the heating medium. He showed that the overall heat transfer coefficient (U) ranging from 570-850 W/m2°C.

Parker (1965) reported the variation in the value of overall heat transfer coefficient for a thin film scraped surface evaporator (TFSSE) between 1134 and 1985 W/m2.°C.

Sangrame et al. (2000) studied the concentration of tomato pulp in a thin film scraped surface evaporator; the main body of the evaporator was 1.4 m high and 0.22 m in diameter. They found that for water as the feed, the overall heat transfer coefficient and evaporation rate ranged within 476.9-939 W/m2.°C and 14.7-30.7 kg/h, respectively For tomato pulp, overall heat transfer coefficient, evaporation rate and final concentration (from 5.9% total solid initial concentration) were varied between 625.6- 910.9 W/m2.°C, 13.22-33.72 kg/h and 8.02-19.21 % TS, respectively. The range of operating parameters were: feed flow rate 40.8-51.0 kg/h, steam temperature 65-80 °C and rotor speed 355 rev/min. The optimum process parameters for the concentration of tomato pulp at 355 rpm rotor speed were found to be 40.3 kg/h feed flow rate and 73 °C steam temperature. The optimum process parameters could give 840 W/m2.°C overall heat transfer coefficient, 27 kg/h evaporation rate and 18 % total solids.

Chuaprasert et al. (1999) and Chawankul et al. (2001) studied the steady state simulation of concentrating sugar syrup and orange juice respectively in ATFE using AspenPlus simulation program to develop the needed model. A rigorous heat exchanger model, Heatx followed by the rigorous 2-phase flash model, flash2, was used to simulate the dominant effects of the ATFE.

The heat exchanger model was used to simulate the evaporator and required the heat transfer area (A), and the overall heat transfer coefficient (U). The output stream from the heat exchanger, a 2-phase stream consisting of concentrated orange juice and waster vapor, was fed to the 2-phase flash unit operating at the same pressure. The thermo-physical properties of both systems were not available in the Aspen Plus databank. They were therefore, determined experimentally and modeled as function of temperature and solid content. Heat transfer coefficients were predicted using correlations and measured from process measurements. Experimental and simulation results were compared and showed good agreement.

MATHEMATICAL TREATMENT

Several assumptions are taken in order to facilitate the mathematical treatment used in the development of the simulation software. These assumptions are summarized as follows:

* Steady state operation.
* Plug flow unit with no backmixing and no radial mixing.
* Adiabatic Mode of Operation.
* Negligible Energy Input from the rotating wiper blades.

44

The wiped-film evaporator for concentration of glycerol-water solution is divided into two sections according to the primary phenomenon occurring therein: sensible heating of the solution, and vaporization of water. The governing material and enthalpy balance equations for each of these sections are presented below (Smith & Van Ness, 1987).

In the sensible heating section, the solution stream is heated from its feed temperature to its initial boiling point; no phase change in this section and no change in the mass flow rate of solution stream occur. In an enthalpy balance about a (dz) increment in this section:

$$\text{Rate of Input} = H + dq \tag{2}$$

$$\text{Rate of Output} = H + \frac{dH}{dz}\,\delta z \tag{3}$$

$$\text{Where} \quad H = WC_P(t - t_R),$$

$$\text{And} \quad dq = U_i\,\pi D_i(t_s - t)\delta z$$

With no accumulation term, the rate of input must equal the rate of output, and the differential enthalpy balance equation is

$$dq - \frac{dH}{dz}\delta z = 0 \tag{4}$$

Or

$$U_i\,a_i(t_s - t)dz - \frac{d\big[WC_p(t - t_R)\big]}{dz}\,dz = 0 \tag{5}$$

Neglecting any change in Cp over a dz increment and recognizing that tR = constant then

$$U_i\,\pi D_i(t_s - t) - WC_p\frac{dt}{dz} = 0 \tag{6}$$

Equation (6) can be integrated analytically between the limits of t = tF and t = tBP if Ui and Cp are assumed constant over this interval. Admittedly this is not true, but the height or length of the preheating zone is quite small, which is generally less than 10% of the total height or length of the heat transfer zone, in the proposed applications. Hence, average values of Ui and Cp based upon their values at the feed temperature and at the initial boiling point can be used in the equation. Integration of this equation then yields:

$$\Delta z = \frac{W\,Cp}{U_i\,\pi D_i}\,\ln\left(\frac{t_s - t_f}{t_s - t_{Bp}}\right) \tag{7}$$

Equation (7) thus determines the required height or length (z) of the preheating section.

Once boiling commences, the boildown ratio function developed previously enters into the calculations. The temperature of the solution stream is incremented in uniform step sizes of (t). The mass flow rate in (kg/h) of this stream at any temperature greater than the initial boiling point is computed from the boildown ratio as follows:

$$W = \frac{\rho\,F_{25}}{BDR} \tag{8}$$

and

$$F_{25} = \frac{\rho_F\,F}{\rho_{25}} \tag{9}$$

The rate of water vaporized over the Δz increment corresponding to the temperature increase Δt is then given by:

$$\Delta V = W_{(t)} - W_{(t+\Delta t)} \tag{10}$$

The enthalpy balance equation in this section has one additional output term (Smith & Van Ness, 1987).

$$\text{Rate of Input} = H + q \tag{11}$$

$$\text{Rate of Output} = H + \left(\frac{dH}{dz}\right)\delta z + rH_v\,\delta z \tag{12}$$

where

$$r = \frac{dV}{dz} = -\frac{dW}{dz} \tag{13}$$

Subtracting the output term from the input term and equating the difference to zero,

$$q - \left(\frac{dH}{dz}\right)\delta z - rH_v\,\delta z \tag{14}$$

Or

$$U_i\,a_i(t_s - t)\delta z - \frac{d\big[WC_p(t - t_R)\big]}{dz}\,\delta z - rH_v\,\delta z = 0 \tag{15}$$

45

Again neglecting any change in C_p over an increment then:

$$U_i \, a_i \left(t_s - t \right) - W C_p \frac{dt}{dz} - C_p \left(t - t_R \right) r - r H_v = 0 \quad (16)$$

Thermodynamically, however, for water

$$H_v - C_p \left(t - t_R \right) = \lambda \quad (17)$$

Where (λ) is the heat of vaporization of water at the temperature t.

Equation (16) can then be rewritten as

$$U_i \, a_i \left(t_s - t \right) - W C_p \frac{dt}{dz} - r \lambda = 0 \quad (18)$$

Using average values of the variable values of U_i, W, C_p and λ, based upon their values at beginning and end of the finite Δt increment, then equation (19) can be written in the following finite difference form:

$$\Delta z = \frac{\overline{W \, C_P} \, \Delta t}{\overline{U_i} \, a_i \left(t_s - \overline{t} \right) - \overline{\lambda} \, r} \quad (19)$$

Finally, after approximating r with $\dfrac{\Delta V}{\Delta z}$, equation (20) can be solved to yield the

$$\boxed{\Delta z = \frac{\overline{\lambda} \, \Delta V + \overline{W \, C_P} \, \Delta t}{\overline{U_i} \, a_i \left(t_s - \overline{t} \right)}} \quad (20)$$

This equation determines the increment height or length required to heat up the vaporized solution stream from t to (t+Δt) at which water is vaporized at the rate of ΔV kg/h.

Experimental Work

The liquids used in this work are non-ionic water supplied from Al-Mansour Factory and glycerol from Vegetable Oils Company. Different concentrations (10, 30, and 50 wt % glycerol solutions) were prepared by weighing method. Liquid viscosities varied from 0.6-135.5 mPa.s, these values were measured using a Fann V-G meter (Baroid) at 50 °C, which was applicable for this range. Liquid densities varied from 985-1240 kg/m3. These values were found by measuring the mass of a known volume (Pycnometer) at 50 °C.

Saturated steam, supplied from a fire tube steam generator, with different pressure (2-5 atm) was used as the heating media in the jacket of the evaporator.

Tap water (flowing at a pressure of 2 atm gauge and ambient temperature) was used as the cooling media in heat exchanger, sealing ring of the vacuum pump and the rotary shaft.

Experiments were carried out in wiped film evaporator supplied from ALVAL Engineering Company. The evaporator consisted from the following parts:

-Main body of evaporator (STRATAVAP Model 8005).
-Graduated glass bottom.
-Separator cyclone.
-Condenser.
-Knock-out pot.
-Rotor drives (STRATAVAP Rotor).
-Vacuum pump (water ring sealing type).
-Different types of pumps for transfer solutions.

The equipment was erected on a steel structure supplied with an electrical board for controlling and operating the different parts of the system. The system's utilities included steam supply, electrical stock and cooling water for sealing and cooling were all connected to the system.

The main body of evaporator consisted of a jacketed cylinder with an inside diameter of 25 cm and active length of 116 cm made of stainless steel 316 L; the jacket was made from the same material with steam inlet pipe and outlet pipe for the condensate. The steam feeding pipe to the jacket had an inside diameter of 2.54 cm made from carbon steel with a regulating valve to control the pressure of steam in the jacket. As for the outlet pipe, it was made from carbon steel having the same diameter connected to a steam trap to permit the condensate steam only to exit from the jacket.

In the top of main body of the evaporator a motor with a gearbox was installed to reduce the speed, fitted with belts to transfer rotation from motor to rotor parts of evaporator. The rotor part consisted of a shaft along the active part of the evaporator with a hung wiper equipped vertically to the shaft. A mechanical seal in the entrance of the shaft to the system existed to prevent the leakage of gases and vapors from the evaporator. At the end of evaporator a graduated glass dish bottom end was installed to collect the produced concentrated solution.

Table 1 Experimental Result.

Run No.	Feed Conc. (Wt. %)	Pressure Depression (mmHg)	Steam Pressure (atm)	Feed Flow Rate (l/h)	Final concentration (Wt %)
1.	10	40	4	50	95
2.	10	40	4	30	98.5
3.	10	100	4	80	94
4.	10	100	4	100	89
5.	10	180	4	120	41
6.	30	40	4	30	99.4
7.	30	40	4	50	99.5
8.	30	120	4	100	95
9.	10	60	2	30	97
10.	10	100	2	50	94
11.	10	100	2	80	58
12.	10	180	2	100	26
13.	50	40	4	80	99.1
14.	50	40	4	100	99

46

Results and Discussion

The effect of operating parameters on the performance of wiped film evaporator was studied using a simulation software. The studied parameters included: pressure depression, saturated steam pressure and feed volumetric flow rate. Experiments were performed using different concentrations of glycerol-water solution (10-50 wt. %) and different feed flow rate (30-120 l/h). The results of the experiments conducted in the present study are given in table(1).

The simulation program was proven to be successful by comparing with randomly selected practical experiments. Where statistical analysis showed that the average absolute error, F-test and correlation coefficient of 2.25%, 0.997 and 0.964 respectively.

During the experimentation and analysis, two distinct zones were recognized; preheating and evaporation. The preheating zone did not exceed 10% of the total evaporator length for all cases studied.

Effect of Pressure Depression

Five levels of pressure depression were chosen; these values were 80,120,160,200 and 400 mm Hg (for a rotation speed of 480 rpm and a steam pressure of 4 atmospheres).

The effect of pressure depression on the final concentration of glycerol and the influence of feed volumetric flow rate is shown in figure (1). It can be seen, as it should be, that the final concentration of glycerol increases with increasing the vacuum, i.e. lowering pressure depression. As the flow rate is increased the effect of pressure depression seems to be less effective. A decrease in the final concentration is noticed as the flow rate is increased (beyond 50 l/h) for all pressure depression levels , but it was , practically, constant below that. Similar results were obtained by Chawankul et al (2001) who studied the concentration of orange juice experimentally and compared the results with a simulation software using ASPEN PLUS.

Figure (2) shows the axial distribution of the overall heat transfer coefficient at the two extreme values of pressure depression used (80 and 400 mm Hg) for a feed flow rate of 100 l/h, a rotation speed of 480 rpm and a steam pressure of 4 atmospheres. It can be seen that the overall heat transfer coefficient increased with increasing pressure depression and a maximum value was noticed at the point separating the preheating zone from the vaporization zone (5-10 cm. from entry). This is due to the decrease in the thermal conductivity of vapors compared to liquids.

Effect of Steam Pressure

The effect of steam pressures (2, 3, 4 and 5 atm.) on the final concentration for different flow rates is shown in figure (3). These results were obtained at 480 rpm and 80 mm Hg pressure depression. It can be observed that the final concentration increased with increasing steam pressure due to the increase of the temperature difference between the utility side (steam side) and the feeds side that caused enhancement of the evaporation rate. At low feed flow rate (below 50 l/h) the effect of steam pressure was not significant but increasing the feed flow rate beyond 100 l/h had caused the effect of steam pressure to be less pronounced.

Comparison of the effect of steam pressure with that of pressure depression, show that the effect of the latter, as expected, is sharper and more significant.

Figure (4) shows the axial distribution of the overall heat transfer coefficient at the extreme cases of steam pressure used (2 and 5 atm.). The results show that the overall heat transfer coefficient increased with decreasing steam pressure; this is due to the fact that at the lower pressure, the temperature difference is larger.

Effect of Rotation Speed

Figure (5) illustrates the effect of the speed of rotation and feed flow rate on the final concentration of glycerol. Results indicate that increasing the feed flow rate caused in decreasing the final glycerol concentration and that increasing the speed of rotation caused significant increase in the final concentration; this increase was noticed to be lower at high feed flow rate. Similar results were found by Komori et al (1988).

The effect of the speed of rotation on the axial distribution of the overall heat transfer coefficient is illustrated in figure (6). The figure show that the heat transfer coefficient reached a maximum at the point separating the preheating zone from the evaporation zone and it increased with increasing the speed of rotation. However the effect of the rotational speed was found to be less pronounced than the other parameters considered. These results were obtained for 480 rpm, 4 atm steam pressure and 100 l/h feed flow rate.
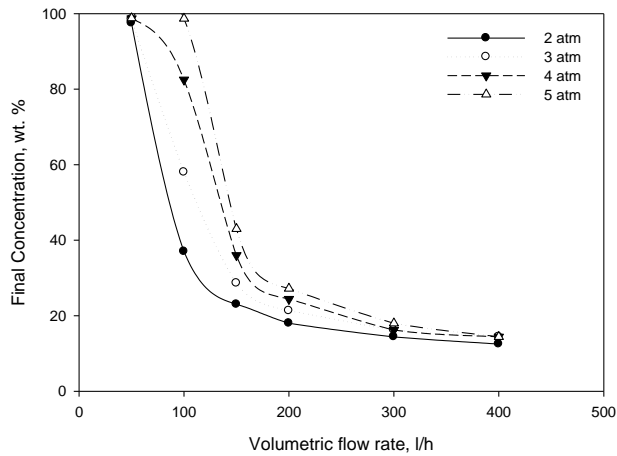
Fig. 1: Final concentration varies flow rate at different pressure depression
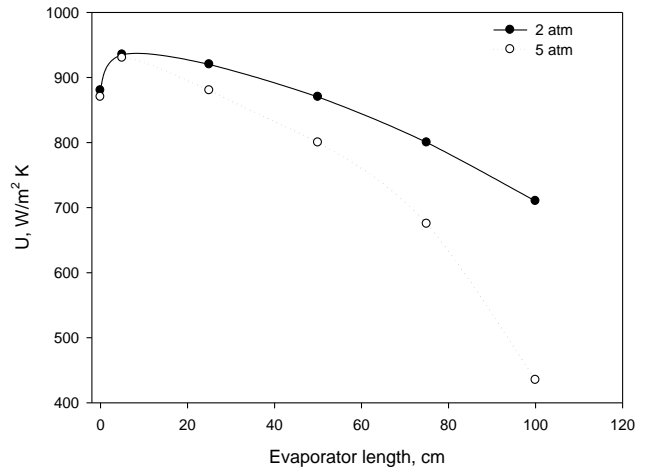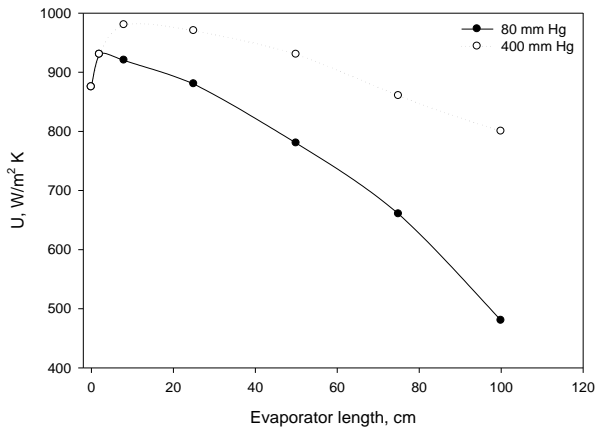

Fig. 2: Axial distribution of over all heat transfer coefficient at different pressure dispersion (Feed flow rate =100 l/h)

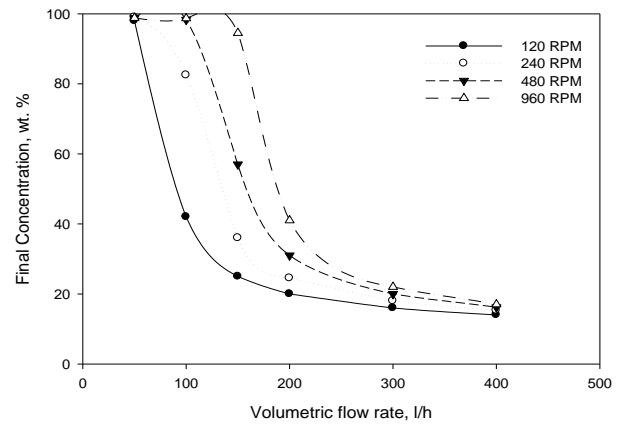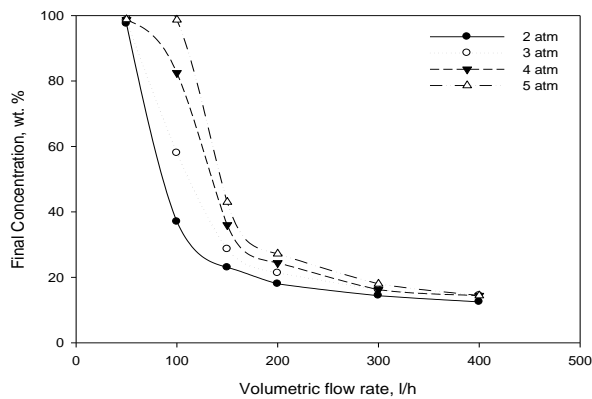Fig. 3: Final concentration versus flow rate at different steam pressure

Fig. 4: Axial distribution of overall heat transfer coefficient at different steam pressure (feed flow rate = 100 l/h)

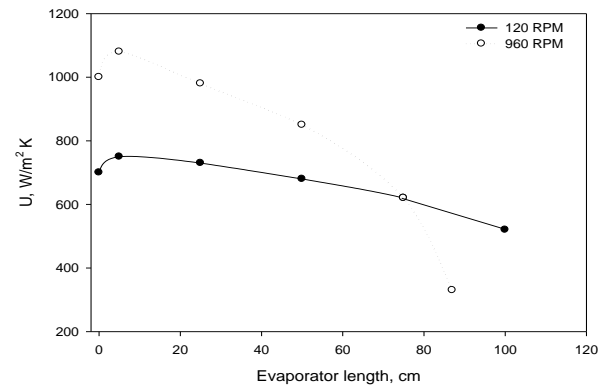Fig. 5: Final concentration versus flow rate at different RPM

Fig. 6: Axial distribution of overall heat transfer coefficient at different RPM (feed flow rate = 100 l/h)

CONCLUSIONS

The required height or length (Δz) of the preheating section was shown to be estimated using equation (7).

The equation that determines the increment height or length required to heat up the vaporized solution stream from t to (t+Δt) at which water is vaporized at the rate of ΔV kg/h is given by equation (20).

The success in applicability of the designed simulation program was proven by the comparison with randomly selected practical experiments. Statistical analysis of the comparison showed that the average absolute error, correlation coefficient and F-test were 2.253 %, 0.997, and 0.964 respectively.

Two distinct zones of operation were observed; preheating and evaporation. And at the point of separation of these two zones the value of heat transfer coefficient reached a maximum. The range of the overall heat transfer coefficient observed in this study was 176-1263 W/m^2 ^{0}K.

Increasing the pressure depression decreased the final concentration of the product but increased the heat transfer coefficient.

Altering the steam pressure did not affect the final concentration significantly, but increasing it caused a lowering in the value of the heat transfer coefficient.

Increasing the speed of rotation increased the final concentration and, also, increased the heat transfer coefficient, where a 66% increase was observed when increasing the speed from 120 to 960 rpm.

Nomenclature

a : Heat transfer area		m^2
BDR : Boil down ratio		---
C_p : Specific heat of fluid		kJ/kg ^{0}K
D : Column diameter		m
F : Mass flow rate		kg/s
h : Heat transfer coefficient		kJ/m^2 s ^{0}K
H : Heat input by flow of fluid stream		kJ/s
K : Thermal conductivity		kJ/m^3 s ^{0}K
L : Thickness		m
q : Heat input by conduction through wall		kJ/s
r :Defined by equation (13)		kg/ms
t : Temperature		$^{\circ}$K
U : Overall heat transfer coefficient		kJ/m^2 s ^{0}K
V : Rate of vaporization		kg/s
W : Flow rate defined by equation (8)		kg/s
z : Column height		m

Greek Letters

λ : Latent heat of vaporization		kJ/kg
ρ : Density		kg/m^3
π : Pi		----

Subscripts

Bp : Boiling point

F : Fluid

i : Inside

o : Outside

R : Reference

s : Steam

v : Vapour

w : Wall

25 : At 25 $^{\circ}$C

REFERENCE

1. Abichandani H., Sharma S.C., and Heldman D.R., (1987) "**Hydrodynamics and Heat Transfer in Thin Film Scraped Surface Heat Exchanger: A Review**", Journal of Food Process Engineering, 9, 143-172.
2. APV Company, "**Evaporator Handbook**", (2000) 4th Edition, EHB-955, www.apv.com.
3. Chawankul N., Chuaprasert S., Douglas P.L. and Luewisutthichat W., (2001) "**Simulation of an Agitated Thin Film Evaporator for Concentrating Orange Juice Using AspenPlus**", Journal of Food Engineering, 47, 4, 247-253.
4. Chuaprasert, S., P. L. Douglas, M. Nguyen, (1999)"**Data Reconciliation of an Agitated Thin Film Evaporator System Using AspenPlus**", J. of Food Engineering, 39, 261-267.
5. Coulson J. M., and Richardson J. F., (1983) "**Chemical Engineering Vol. 2**", 3rd Edition, Pergamon Press .
6. Freese H.L., and Glover, W.B., (1979) "**Mechanically Agitated Thin-Film Evaporators**", Chem. Eng. Pro. , Jan., 52-58.
7. Mutzenburg A. B., (1965) "**Agitated Thin-Film Evaporators, Part.1: Thin Film Technology**", Chem. Eng. 72 (19), 175-178.
8. Parker N., (1965) "**Agitated Thin-Film Evaporators, Part.2: Equipment's and Economics**", Chem. Eng., 72 (19), 179-185.

9. Sangrame, G., Bhagavathi, D., Thakare, H., Ali, S. and Das, H., (2000) "**Performance Evaluation of a Thin Film Scraped Surface Evaporator for Concentration of Tomato Pulp**", J. Food Eng., 43, 205-211.

10. Smith J.M. and Van Ness H.C., (1987) "Introduction to Chemical Engineering Thermodynamics", 4th Edition, McGraw-Hill Book Company, New York.